Calculation of period doubling in a Josephson circuit

Kurt Wiesenfeld and Edgar Knobloch
Department of Physics, University of California, Berkeley, California 94720

Robert F. Miracky and John Clarke
Department of Physics, University of California, Berkeley, California 94720
and Materials and Molecular Research Division, Lawrence Berkeley Laboratory, Berkeley, California 94720
(Received 14 November 1983)

The method of harmonic balance is used to obtain analytic results for the differential equation describing a current-biased Josephson junction with self-capacitance that is shunted by a resistor with substantial self-inductance. This system is known to exhibit period-doubling cascades, chaos, and other exotic nonlinear phenomena. After an accurate representation of the basic voltage oscillation is determined for high-bias currents, the value of bias current is computed for which this solution loses stability to a period-doubled mode. The predictions agree to remarkable accuracy with results obtained from both analog simulations and digital integration of the circuit equation, typically 5% for moderate values of inductance. Moreover, the method of calculation provides a systematic scheme for achieving increasing accuracy.

I. INTRODUCTION

There has recently been considerable interest in the nonlinear dynamics of Josephson junctions[1] driven by steady and/or alternating currents.[2–16] Under appropriate conditions, these devices exhibit period-doubling sequences, chaos, intermittency, relaxation oscillations, and hopping between metastable states. Much of this work has been directed towards a junction shunted by its self-capacitance and a resistor and driven by an alternating current.[4–7,10–13] This system is governed by the same second-order nonautonomous equation as the driven pendulum, namely,

$$\ddot{\delta}+\gamma\dot{\delta}+\Omega_0^2\sin\delta=A\cos(\omega t)\ . \tag{1}$$

There has been little experimental investigation of this system with real Josephson junctions, but considerable work has been done using analog simulations and digital computers. There have also been efforts to study this equation analytically.[5,12,13] Levinsen[12] replaced $\sin\delta$ with $\delta-\delta^3/6$, an approximation that is valid only for small δ, and that does not allow one to study running solutions. However, one can predict the value of A for which the solution first contains even-harmonic components.[17] Pedersen *et al.*[5] have analyzed Eq. (1) retaining the full sine nonlinearity. They conclude that their approximations yield only a qualitative guide to understanding the experimental results. On a more formal level, Odyniec and Chua[13] have been able to make statements concerning the existence of periodic and aperiodic solutions to Eq. (1).

In this paper, we are concerned with a different system, namely, a Josephson junction shunted by its self-capacitance and by an inductance in series with a resistor, and biased with a steady current. This system, which is described by a third-order autonomous ordinary differential equation [see Eq. (8)], has been studied in detail both experimentally[14,16] and by means of analog simulations and digital computations.[18] Using analytic methods[19,5] similar to those previously employed to study Eq. (1), we find results for high current biases that are in quantitative agreement with those obtained by both analog and digital means. Furthermore, we can predict the value of the current at which the period-doubling instability occurs for a given set of junction parameters.

In Sec. II we derive the equation of motion and construct a solution using the method of harmonic balance. We compare this solution with the results of both analog simulations and digital computations. The onset of period doubling is analyzed in Sec. III, and further bifurcations are discussed in a more heuristic fashion in Sec. IV. Section V contains a discussion of the results. The methods used in the digital computation and analog simulation will be described in detail elsewhere.[18]

II. EQUATION OF MOTION

The Josephson tunnel junction consists of two superconductors separated by a thin insulating barrier through which pairs of electrons (Cooper pairs) are able to tunnel coherently; the flow of pairs thus constitutes a supercurrent. When an external current I is applied, no voltage appears until the critical current I_0 is exceeded. The supercurrent is equal to $I_0\sin\delta$, where δ is the difference in the phases of the order parameters on either side of the barrier. When there is a voltage V across the junction the phase difference evolves with time according to the relation $\dot{\delta}=2eV/\hbar$, where e is the electronic charge, $2\pi\hbar$ is Planck's constant, and the dot implies differentiation with respect to time. The tunnel junction is shunted by its self-capacitance C and by a conductance that allows a quasiparticle current I_{qp} to flow in the presence of a voltage. In the device of interest here, an external shunting resistance R is added which has a self-inductance L. The

resulting circuit is shown in Fig. 1, and is governed by the equations

$$I = I_0 \sin\delta + \frac{\hbar C}{2e}\ddot{\delta} + I_S + I_{qp} \tag{2}$$

and

$$\frac{\hbar}{2e}\dot{\delta} = I_S R + L\dot{I}_S + V_N \ , \tag{3}$$

where V_N is the thermal voltage noise generated by the resistance R. If we introduce a dimensionless time variable

$$\tilde{t} = (2\pi I_0 R/\Phi_0)t \ , \tag{4}$$

where $\Phi_0 \equiv h/2e$ is the flux quantum, Eqs. (2) and (3) become

$$i = \sin\delta + \beta_C\ddot{\delta} + i_S + i_{qp} \tag{5}$$

and

$$\dot{\delta} = i_S + \beta_L\dot{i}_S + v_N \ , \tag{6}$$

with

$$\begin{aligned} &i \equiv I/I_0, \quad i_S \equiv I_S/I_0, \quad i_{qp} \equiv I_{qp}/I_0 \ , \\ &v_N \equiv \frac{V_N}{I_0 R}, \quad \beta_C \equiv \frac{2\pi I_0 R^2 C}{\Phi_0}, \quad \beta_L \equiv \frac{2\pi L I_0}{\Phi_0} \ . \end{aligned} \tag{7}$$

The dot now denotes differentiation with respect to $\tilde{t}$.

Neglecting the quasiparticle current and the noise voltage, we combine Eqs. (5) and (6) to give the third-order equation

$$\beta_L\beta_C\dddot{\delta} + \beta_C\ddot{\delta} + \dot{\delta}(1+\beta_L\cos\delta) + \sin\delta = i \ . \tag{8}$$

The system is seen to depend on three dimensionless parameters: β_L, β_C, and i. Note that in the absence of driving terms, Eqs. (1) and (8) both possess the symmetry $\delta \rightarrow -\delta$. In the latter equation, the symmetry is broken by the dc term. This difference between Eqs. (1) and (8) has important consequences for the observed dynamics.

A crucial observation is that for high enough bias current i, the voltage across the junction consists of a large dc offset plus a small amplitude oscillation, regardless of the values of β_L and β_C. Physically, this is because most of the bias current flows through the resistor, so the junction approaches a voltage biased limit characterized by sinusoidal current oscillations. As β_C is increased, the absolute amplitude of the residual voltage oscillation decreases even more rapidly as the bias current is increased, due to the presence of the capacitance which shunts alternating current. As i is lowered from a high value, this basic oscillation grows in amplitude and the dc component decreases. Eventually, this solution becomes unstable to a new mode. We wish to represent this high-i solution analytically, and to compute when it loses stability.

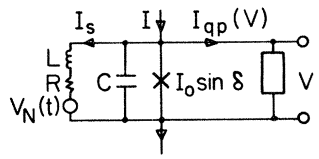

FIG. 1. Schematic representation of Josephson tunnel junction with critical current I_0 and self-capacitance C shunted with an external resistance R which has a self-inductance L; I_{qp} is the quasiparticle tunneling current and V_N is the Nyquist voltage noise of the resistance.

Since the voltage is proportional to $\dot{\delta}$, we put

$$\dot{\delta} = \bar{v} + \dot{x}(\tilde{t}) \ , \tag{9}$$

where $\bar{v}$ is some constant, and x is a periodic function of time. Also, we introduce a new time

$$\tau \equiv \bar{v}\tilde{t} \ . \tag{10}$$

Taken together, Eqs. (9) and (10) imply

$$\delta' = 1 + x' \ , \tag{11}$$

where the primes denote differentiation with respect to τ.

With these changes, the governing equation (8) may be written

$$\begin{aligned} &\beta_L\beta_C\bar{v}^3 x''' + \beta_C\bar{v}^2 x'' + \bar{v}x' \\ &\quad + \bar{v}\beta_L[\sin(\tau+x)]' + \sin(\tau+x) = i - \bar{v} \ . \end{aligned} \tag{12}$$

Although we have been motivated by the known behavior for large i, we have made no assumptions about the relative size of the terms appearing in (12).

Equation (12) may now be tackled by the method of harmonic balance,[19] which is closely related to the method of Fourier series used for linear equations. Assuming that x is periodic, we write

$$x(\tau) = \sum_{n=1}^{\infty} A_n \sin(n\tau + \phi_n) \ , \tag{13}$$

where A_n and ϕ_n are constants to be determined.

After substituting this into Eq. (12), we balance coefficients of each Fourier mode independently. This procedure leads to an infinite set of algebraic equations. If Eq. (12) were linear with constant coefficients, these would be uncoupled, linear equations. However, Eq. (12) instead generates an infinite set of coupled, nonlinear (transcendental) algebraic equations. The method of harmonic balance amounts to arbitrarily truncating the expansion, Eq. (13), and ignoring higher harmonics generated by the nonlinearities in Eq. (12).

For example, the crudest approximation is obtained by including only a single term of (13):

$$x(\tau) = A_1 \sin(\tau + \phi_1) \ , \tag{14}$$

so that

$$\delta = \tau + A_1 \sin(\tau + \phi_1) \ . \tag{15}$$

Now,

$$\begin{aligned} &\sin[\tau + A_1\sin(\tau+\phi_1)] \\ &\quad = \sum_{m=-\infty}^{\infty} J_m(A_1)\sin[(m+1)\tau + m\phi_1] \ , \end{aligned} \tag{16}$$

where J_m is the mth-order Bessel function of the first kind. Consequently, substitution of Eq. (14) into Eq. (12)

TABLE I. Values of Bessel functions J_m of argument A_1.

A_1	J_0	J_1	J_2	J_3	J_4
0.2	0.990	0.100	0.005	$<10^{-3}$	$<10^{-5}$
0.6	0.912	0.287	0.044	0.004	$<10^{-3}$
1.0	0.765	0.440	0.115	0.020	0.002
1.4	0.567	0.542	0.207	0.050	0.009

yields terms of *all* harmonics. The justification for ignoring all these higher harmonics is that for $A_1 \lesssim 1$, $|J_m(A_1)|$ is a rapidly decreasing function of $|m|$ (see Table I). In the parameter range considered, A_1 is not bigger than about 0.7.

Thus, for x given by Eq. (14), Eq. (12) generates three equations, obtained by separately balancing constant terms, those proportional to $\sin\tau$, and those proportional to $\cos\tau$. Omitting the detailed algebra, these are

$$J_1 \sin\phi_1 = i - \bar{v} , \tag{17}$$

$$A_1\bar{v}(1-\beta_L\beta_C\bar{v}^2)+\bar{v}\beta_L(J_0-J_2)\cos\phi_1-(J_0+J_2)\sin\phi_1=0 , \tag{18}$$

and

$$\beta_C\bar{v}^2A_1-\bar{v}\beta_L(J_0+J_2)\sin\phi_1+(J_2-J_0)\cos\phi_1=0 , \tag{19}$$

where the Bessel functions J_m are evaluated at A_1.

Given β_L, β_C, and i, these equations may be solved for $\bar{v}$, A_1, and ϕ_1. Careful numerical analysis of Eqs. (17)—(19) shows that this solution is unique.

Figure 2 compares the results from an analog circuit with the values of $\bar{v}$ and A_1 obtained from Eqs. (17)—(19). (The angle ϕ_1 is not a measured quantity.) Also shown are the results of integrating the evolution equation (8) directly on a digital computer. It is seen that the calculations reproduce remarkably well the values obtained from the digital computer, agreeing to within 1% over a wide range of parameter values. The analog circuit also gives 1—2 % agreement for the quantity $\bar{v}$, while there is a systematic discrepancy of about 10% for the amplitude A_1. In both cases, the disagreement can be accounted for by the uncertainties involved in the measurements.

As already mentioned, Eq. (14) is the crudest representation of the oscillation. Of course, the method of harmonic balance gives us a systematic scheme of approximation. One expects the fit to improve as more terms in Eq. (13) are retained. If we use

$$x(\tau)=A_1\sin(\tau+\phi_1)+A_2\sin(2\tau+\phi_2) \tag{20}$$

instead of Eq. (14) we find five coupled algebraic equations for $\bar{v}$, A_1, A_2, ϕ_1, and ϕ_2. We omit displaying these equations in the interest of brevity, but remark that they reduce to Eqs. (17)—(19) if one sets $A_2=0$ and $\phi_2=0$. A particularly interesting question is whether this calculation gives the proper amount of higher-harmonic content of the voltage signal. Figure 3 compares the ratio A_2/A_1 from this calculation with that obtained for the analog simulation from a power spectrum analyzer. The agreement is quite good. Furthermore, we may conclude that the calculation is self-consistent: Figure 3 shows that $A_2/A_1 \ll 1$.

III. STABILITY ANALYSIS

To test the stability of the basic oscillation, one examines the evolution of an orbit infinitesimally close to this solution. Thus we substitute

$$\delta=\delta_0+\xi \tag{21}$$

into Eq. (8), where δ_0 is the solution found in Sec. II and ξ is an infinitesimal perturbation. The resulting *linearized* equation for ξ is

$$\bar{v}^3\beta_L\beta_C\xi'''+\bar{v}^2\beta_C\xi''+\bar{v}\xi'+\bar{v}\beta_L(\xi\cos\delta_0)'+\xi\cos\delta_0=0 . \tag{22}$$

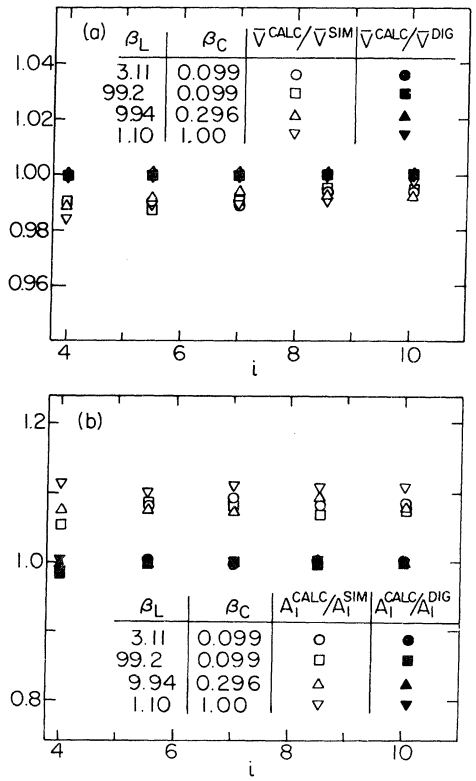

FIG. 2. Comparison of harmonic balance calculations with analog simulations (open symbols) and digital computations (closed symbols) for a variety of parameter values. Results shown for (a) mean voltage $\bar{v}$ and (b) amplitude of phase oscillation A_1.

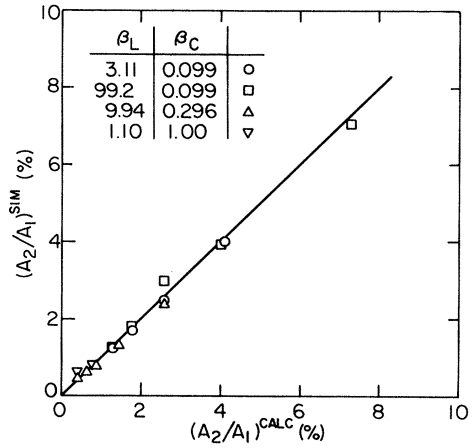

FIG. 3. Ratio of second-harmonic amplitude A_2 to first-harmonic amplitude A_1 for analog simulations vs harmonic balance calculations.

Equation (22) is a linear ordinary differential equation with periodic coefficients. Floquet's theorem[19] guarantees the existence of nontrivial solutions such that

$$\xi(\tau+T)=\mu\xi(\tau)\ , \tag{23}$$

where μ is a (possibly complex) constant and T is the least period common to the coefficients in Eq. (22)—for our case $T=2\pi$. In fact, since Eq. (22) is a third-order ordinary differential equation, we expect three such multipliers μ, though they need not be distinct. The solution δ_0 is orbitally stable provided that the perturbation ξ does not grow in magnitude. In that case, all the multipliers must satisfy

$$|\mu|<1\ . \tag{24}$$

As the parameters of our system are varied, the multipliers move around in the complex plane. An instability is signaled when one of the multipliers crosses the unit circle. There are three possibilities.

(i) Some μ passes through -1. From Eq. (23), it is clear that $\mu=-1$ corresponds to a period-doubled solution.

(ii) Some μ passes through $+1$. This corresponds to an instability of the same period as the original oscillation.

(iii) A complex-conjugate pair (μ,μ^*) pass through the unit circle. In most cases the resulting orbits are confined to an invariant torus.[20]

We now proceed to examine each of these cases.

A. Period-doubling instability

This corresponds to case (i) above. When the relevant multiplier μ is precisely equal to -1, there is a solution of period 4π satisfying Eq. (22). To find when such a solution occurs, we again use the method of harmonic balance. Let

$$\xi(\tau)=\gamma_0+\sum_{m=1}^{\infty}\left[\gamma_m\cos\frac{m\tau}{2}+\alpha_m\sin\frac{m\tau}{2}\right]\ . \tag{25}$$

Substituting Eq. (25) (along with the assumed-known Fourier decomposition for δ_0) into Eq. (22), and balancing the coefficients for each harmonic, we find a system of coupled linear homogeneous algebraic equations.

Observe, however, that this system decomposes into two disjoint subsystems. For, suppose Eq. (25) is restricted to integer harmonics. Equation (22) couples harmonics via the product of $\cos\delta_0$ and ξ. Since $\cos\delta_0$ contains only integer harmonics, this product generates only integer harmonics again. This even-m expansion for ξ corresponds to a solution with the same period as δ_0, and is considered further in Sec. III B.

In contrast, for the expansion

$$\xi(\tau)=\sum_{m\ \text{odd}}\left[\gamma_m\cos\frac{m\tau}{2}+\alpha_m\sin\frac{m\tau}{2}\right]\ , \tag{26}$$

which represents a bona fide solution of period 4π, the coupling $\xi\cos\delta_0$ yields only noninteger harmonics. This leads to a closed system of algebraic equations for the coefficients of Eq. (26).

Next, we approximate Eq. (26) by retaining the $m=1$ and 3 terms only, and assume (as in Sec. II) that δ_0 is given by

$$\delta_0=\tau+A_1\sin(\tau+\phi_1) \tag{27}$$

to sufficient accuracy. With these approximations, Eq. (22) generates a system of four linear homogeneous algebraic equations for γ_1, α_1, γ_3, and α_3, which may be expressed in the matrix form

$$M\begin{bmatrix}\gamma_1\\ \alpha_1\\ \gamma_3\\ \alpha_3\end{bmatrix}=0\ , \tag{28}$$

where A_1, $\bar{v}$, and ϕ_1 are obtained for any choice of parameters (i,β_L,β_C) by using the procedure of Sec. II. The matrix M is most conveniently expressed as the sum of the three other matrices,

$$M=Q+P+\Lambda\ , \tag{29}$$

where

$$\begin{aligned}
Q_{11}&=\tfrac{1}{2}(J_0+J_2)-J_1\cos\phi_1-J_2\sin^2\phi_1\ ,\\
Q_{12}&=Q_{34}=-\tfrac{1}{2}J_2\sin(2\phi_1)\ ,\\
Q_{13}&=\tfrac{1}{2}[J_0+J_2+(J_1+J_3)\cos\phi_1]\\
&\quad -J_2\sin^2\phi_1-J_3\cos(2\phi_1)\cos\phi\ ,\\
Q_{14}&=Q_{12}-\tfrac{1}{2}(J_1+J_3)\sin\phi_1+J_3\sin(2\phi_1)\cos\phi_1\ ,\\
Q_{22}&=-Q_{11}+2J_1\cos\phi_1\ ,\\
Q_{23}&=Q_{14}+J_2\sin(2\phi_1)\ ,\\
Q_{24}&=-Q_{13}-2J_2\sin^2\phi_1+J_0+J_2\ ,\\
Q_{33}&=-J_1\cos\phi_1+\tfrac{1}{2}J_2\cos(2\phi_1)\ ,\\
Q_{44}&=-J_1\cos\phi_1-\tfrac{1}{2}J_2\cos(2\phi_1)\ ,\\
Q_{ij}&=Q_{ji}\ ,
\end{aligned} \tag{30}$$

$$P_{1j}=\tfrac{1}{2}\bar{v}\beta_L Q_{2j}\ ,$$

$$P_{2j}=-\tfrac{1}{2}\bar{v}\beta_L Q_{1j}\ ,$$

$$P_{3j}=\tfrac{3}{2}\bar{v}\beta_L Q_{4j}\ ,$$

$$P_{4j}=-\tfrac{3}{2}\bar{v}\beta_L Q_{3j}\ ,$$

$$\Lambda_{11}=\Lambda_{22}=\tfrac{1}{9}\Lambda_{33}=\tfrac{1}{9}\Lambda_{44}=-\tfrac{1}{4}\beta_C\bar{v}^2\ ,$$

$$\Lambda_{12}=-\Lambda_{21}=-\tfrac{1}{2}\bar{v}-\tfrac{1}{8}\beta_L\beta_C\bar{v}^3\ ,$$

$$\Lambda_{34}=-\Lambda_{43}=\tfrac{3}{2}\bar{v}-\tfrac{27}{8}\beta_L\beta_C\bar{v}^3\ ,$$

all other $\Lambda_{ij}=0$. The solution of Eq. (28) demands that the determinant of the coefficient matrix vanish, yielding a single condition on the parameters (i,β_L,β_C).

Figure 4 compares the results of this calculation with both digital computations and analog simulations for $\beta_C=0.0986$, giving the critical value of bias current $i=i_{\rm crit}$ for the onset of period doubling for various values of β_L. In order to obtain accurate results, it is important that an accurate representation of δ_0 be used. The figure presents two theoretical curves. The solid line uses the crudest approximation for δ_0, obtained by assuming the existence of only the single harmonic [see Eq. (15)] in the basic oscillation. The dashed-dotted curve (see inset) assumes Eq. (20) to obtain better estimates of A_1, ϕ_1, and $\bar{v}$, but still uses Eq. (27) for the period-doubling part of the calculation. Obviously, these are only the first of a systematic sequence of calculations which should converge to the exact answer. From Fig. 4 we see that good accuracy is already achieved for the crudest approximation, the more refined approach becoming important for higher values of β_L. The first correction accounts for about one-third of the discrepancy between the calculation and the digital integration for $\beta_L=14$.

The results of the analog simulations agree with the results of the digital computations and analytical calculation to a much greater accuracy in Fig. 4 than one might have expected from the results summarized in Fig. 2(b). As this agreement is more consistent with the results in Fig. 2(a), we conclude that it is the oscillation *frequency*, rather than the amplitude, which is of greatest importance in determining when period doubling sets in.

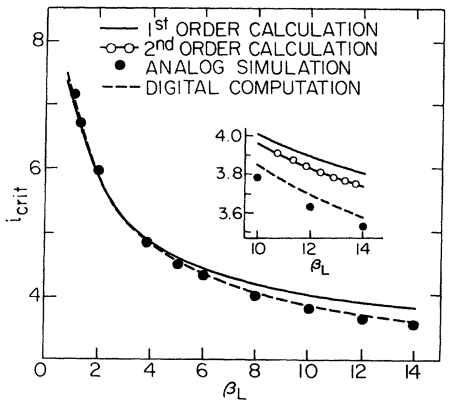

FIG. 4. Onset of period doubling: $i_{\rm crit}$ vs β_L for $\beta_C=0.0986$. Solid curve represents calculations based on the first-order approximation Eq. (14), while the dashed-dotted curve (inset) uses the second-order approximation Eq. (20). Dashed line gives the results of digital computations, while the solid circles are from analog simulations.

An interesting feature predicted by our calculation is that there is a minimum value of $\beta_L=\beta_{L,\min}$ (for fixed β_C) for which the period-doubling instability can occur. This behavior is also observed in the analog simulations. For $\beta_C=0.1$ we find the theoretical value $\beta_{L,\min}=0.72$ as compared with the value determined from the analog simulation $0.77<\beta_{L,\min}<0.84$.

B. Period-one instabilities

We now consider

$$\xi(\tau)=\gamma_0+\sum_{m\ \text{even}}\left[\gamma_m\cos\frac{m\tau}{2}+\alpha_m\sin\frac{m\tau}{2}\right]. \tag{31}$$

We ignore terms with $m\geq 6$, and take δ_0 to be given by Eq. (27). Harmonic balance generates a fifth-order system of linear algebraic equations, which we omit for brevity. A period-one instability would be signaled by the vanishing of the determinant of the 5×5 coefficient matrix. However, we find that, for $A_1\leq 1.0$, the determinant never vanishes.

To summarize, the situation is as follows. For large enough i, δ oscillates according to Eq. (15). As i is gradually decreased, the amplitude A_1 grows. If $\beta_L\geq\beta_{L,\min}$, this solution will lose stability to a period-doubled oscillation at $i=i_{\rm crit}$. If $\beta_L<\beta_{L,\min}$, no period-doubling instability occurs, and A_1 continues to grow as i is lowered. Recall, however, that the truncation of Eq. (13) becomes less reliable as A_1 increases. For $A_1\leq 1.0$, we have verified that this basic solution remains stable with respect to the perturbation, Eq. (31).

C. Hopf instability

We can show that the case where a pair of complex-conjugate multipliers exit the unit circle cannot occur for Eq. (22). Toward this end, we rewrite Eq. (22) in the vector form

$$\frac{d}{d\tau}\begin{bmatrix}\xi\\ \xi'\\ \xi''\end{bmatrix}=\Xi\begin{bmatrix}\xi\\ \xi'\\ \xi''\end{bmatrix}, \tag{32}$$

with

$$\Xi=\begin{bmatrix}0 & 1 & 0\\ 0 & 0 & 1\\ -\dfrac{\bar{v}\beta_L(\cos\delta_0)'+\cos\delta_0}{\bar{v}^3\beta_L\beta_C} & \dfrac{-(1+\beta_L\cos\delta_0)}{\bar{v}^2\beta_L\beta_C} & \dfrac{-1}{\beta_L\bar{v}}\end{bmatrix}. \tag{33}$$

As pointed out by Crawford,[21] a sufficient condition for ruling out the possibility of a Hopf bifurcation for a third-order autonomous system is

$$\int_0^T \mathrm{Tr}\,\Xi(\tau)d\tau<0\ , \tag{34}$$

where T is the period of the limit cycle. From Eq. (33),

we see that the condition given by Eq. (34) is indeed fulfilled, since β_L is necessarily positive. This conclusion is in complete agreement with the analog simulations.

IV. FURTHER (QUALITATIVE) ASPECTS

We have demonstrated that accurate quantitative predictions are in hand for the onset of the first instability of the basic oscillation. The linear stability analysis of Sec. III cannot tell us what happens beyond the instability. This requires finding the new solution from the full nonlinear equation (8). One can well imagine using the method of harmonic balance again to locate the period-doubled oscillation, followed by a stability analysis of this solution, and so on.

However, some further inferences may be gleaned from the work already presented. In particular, consider the analysis of Sec. III A. After i is lowered beyond i_{crit}, the system goes to a new period-doubled solution. Nevertheless, the period-one solution—though unstable—still exists. It may happen that this period-one solution regains stability as i is lowered still further. If this is the case then the determinant of the coefficient matrix appearing in Eq. (28) vanishes a second time. This does indeed occur for certain parameter values.

What can one expect to observe in such a case? In general, one cannot decide simply by studying the stability of the period-one solution. For instance, the period-doubled solution might bifurcate to a more complicated solution which retains stability even after the period-one solution regains stability. The physical system could then operate in either of these coexisting modes, depending on the initial conditions. However, most likely is the situation depicted in Fig. 5. The bifurcation diagram shown is produced from digital computations with $\beta_C=0.1$ and $\beta_L=0.904$ (i.e., for β_L slightly greater than $\beta_{L,\min}$). Here, the local maxima $v_{\max}$ of the voltage oscillations are plotted versus bias current. This figure shows a period-doubling bifurcation which then "reverses itself." (This is reminiscent of Fig. 3 of Ref. 6.) The region containing the bubble corresponds to the existence of a period-doubled solution, which has two distinct values of local voltage maxima. The arrows indicate the values of i where the period-one oscillation loses and then regains stability, as predicted by Eq. (28). For these values of β_L and β_C, A_1 remains reasonably small ($\lesssim 1.0$) in this range of i, so that the agreement is still quite good.

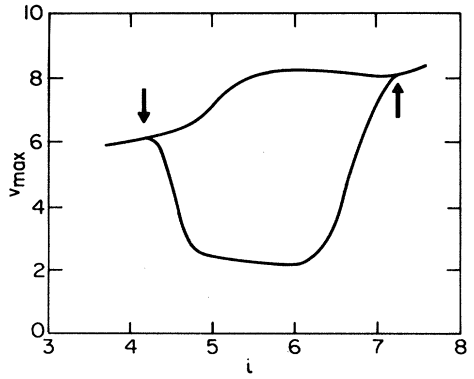

FIG. 5. Bifurcation diagram for $\beta_L=0.904$ and $\beta_C=0.1$, from digital computations. Values of local maxima of observed voltage oscillations are plotted versus i. Arrows indicate where the harmonic balance calculation predicts the period-one oscillation loses and then regains stability.

Finally, consider again the case of $\beta_L<\beta_{L,\min}$. As stated previously, the basic high-i oscillation remains stable as i is lowered. Eventually, the amplitude A_1 grows (as do the higher-harmonic amplitudes A_2, A_3, etc.) to the extent that our truncation Eq. (14) becomes unreliable. As i is lowered past unity, the governing equation (8) has two new fixed-point solutions

$$\delta=\arcsin i, \quad 0\le\delta<2\pi . \tag{35}$$

Linear stability analysis shows that the smaller value of δ is a stable fixed point, the other is unstable. What, if anything, may we say about the time-dependent solution of Eq. (8) in this parameter regime? Physically, for $i<1$, the Josephson junction represents a short circuit at zero frequency—the entire bias current flows through the junction and the (stable) fixed point Eq. (35) is observed. The time-dependent solution is no longer seen. A clue to what is happening is provided by the nature of the transition to the fixed point. As one lowers i, the period of the oscillation increases dramatically before the oscillations disappear at some i less than 1. If i is increased again, the observed solution remains time independent until $i=1$, where a sudden jump to oscillations occurs. The transition is thus strongly hysteretic.

All this suggests the sequence of events depicted schematically in Fig. 6. Here, the orbits in the three-dimensional phase space $(\delta,\dot\delta,\ddot\delta)$ are projected onto a plane. For $i>1$, the only attractor is the periodic orbit [Fig. 6(a)]. (We have made the physically obvious identification for the phase $\delta=\delta+2\pi n$.) For i just under unity, the pair of fixed points Eq. (35) appear in a saddle-node bifurcation [Fig. 6(b)]. Eventually, the unstable fixed point collides with the stable limit cycle, combining to give an infinite-period, homoclinic orbit [Fig. 6(c)]. This kind of bifurcation is called a *global* bifurcation[20,22] in contrast to a local bifurcation such as a saddle node. Glo-

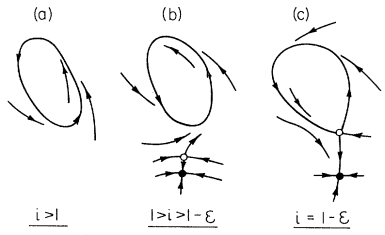

FIG. 6. Sketches of the projection of flow in three-dimensional $(\delta,\dot\delta,\ddot\delta)$ phase space onto the plane for i near unity. (a) Trajectories all approach the stable limit cycle. (b) A saddle-node bifurcation creates a pair of new fixed points. (c) The unstable fixed point collides with the limit cycle, forming a homoclinic orbit via a global bifurcation. ϵ is a small, positive number.

bal bifurcations are much more difficult to study analytically, but their occurrence often heralds very complicated dynamics for nearby parameter values.[20] For the present system, this process is described elsewhere.[23]

V. DISCUSSION

We have made analytic headway on the Josephson junction system of Fig. 1. Quantitatively accurate results for the basic high-i oscillation and for the onset of period doubling have been achieved using the method of harmonic balance. One of the chief virtues of this method is that it gives a systematic approach for finding successively better predictions by including more harmonics in the basic oscillation and/or the perturbations. Moreover, we found that even the simplest possible calculations fit the digital computations extremely well (Figs. 2—4), without benefit of any adjustable parameters.

The governing evolution equation was taken to be Eq. (8), which neglects the quasiparticle current and thermal voltage noise. This restricts a detailed comparison between the present calculation and any experimental realization of the Josephson junction modeled by Fig. 1. However, it seems that an equation that took into account the quasiparticle current could be fruitfully tackled by harmonic balance. After all, this method relies on the oscillation having small higher-harmonic content, a condition well satisfied in the present system (as demonstrated by analog simulations).

Our approach has been essentially the one discussed by Pedersen *et al.*[5] to analyze Eq. (1). As mentioned in Sec. I, those authors did not try to make quantitative comparisons between calculations and experiments. They cited the above limitations of the governing circuit equations, as well as the importance of higher-harmonic content appearing in the voltage oscillations as prohibiting any detailed agreement. Their calculations included only the lowest Fourier mode. On the other hand, the success of the work presented here justifies renewed optimism for getting good quantitative predictions for the system represented by Eq. (1). It seems to us that the most important correction would be to include higher harmonics in the basic oscillation. It is crucial to obtain a good representation of this oscillation, since the search for a period-doubling instability relies on linearizing the evolution equation about this solution. Thus even a small error in the expression for the basic solution could have a large effect on the stability calculations.

Another point to discuss concerns the role of symmetry. Having isolated the large-i solution, linear stability analysis allows us to find the *first* instability as i is lowered—in the present case, a period-doubling instability. In contrast, a recent paper by Novak and Frehlich[17] reported successful predictions for the first instability of the driven Duffing equation. In their case, the instability involved symmetry-breaking rather than period-doubling. For small driving amplitudes A, the basic oscillation has only odd-harmonic content—the first instability as A is increased is to a solution containing both odd and even harmonics. This symmetry-breaking was conjectured to be a necessary precursor for the period-doubling cascade, which is observed as A is increased still further. We want to understand the fundamental reason behind this phenomenon: Essentially, its origin lies in the symmetry of the governing equation. The point is that the symmetry of the equation (and basic oscillation) prevents the first bifurcation from being a period doubling. Consequently, a calculation along the lines presented here must be carried out (at least) to the *second* instability in order to locate the onset of period doubling. In contrast, Eq. (8) is not symmetric, so the first instability *can* be a period doubling.

It is worthwhile to present here a heuristic explanation of how symmetry suppresses period-doubling bifurcations. Our discussion focuses on equations with the symmetry of the driven Duffing equation—hence it applies to Eq. (1) as well—but the argument may be generalized. A general discussion, using the methods of bifurcation theory for mappings, is presented in Ref. 24.

The driven Duffing equation,

$$\ddot{\delta}+\gamma\dot{\delta}+\Omega_0^2\delta+\alpha\delta^3=A\cos t\ , \tag{36}$$

has the symmetry $\delta\rightarrow-\delta$, $t\rightarrow t+\pi$. In other words, if $\delta(t)$ is a solution of Eq. (36), than so is $-\delta(t+\pi)$. These solutions may or may not be distinct. We shall call the solution *symmetric* if

$$\delta(t)=-\delta(t+\pi)\ . \tag{37}$$

Observe that a periodic solution is symmetric if and only if it contains only odd harmonics, as can be seen by looking at the Fourier expansions

$$\delta(t)=\sum_{n\ \text{odd}}A_n\sin(nt+\phi_n)+\sum_{n\ \text{even}}A_n\sin(nt+\phi_n) \tag{38}$$

and

$$-\delta(t+\pi)=\sum_{n\ \text{odd}}A_n\sin(nt+\phi_n)-\sum_{n\ \text{even}}A_n\sin(nt+\phi_n)\ . \tag{39}$$

We now want to show that a symmetric periodic solution (i.e., a symmetric limit cycle) will not lose stability to a period-doubled solution.

As in Sec. III, the stability of a solution δ_0 is studied by linearizing Eq. (36) about δ_0. Suppose we have exactly one Floquet multiplier μ on the unit circle. Then there is a *real* perturbation ξ satisfying

$$\xi(t+2\pi)=\mu\xi(t),\quad \mu=\pm1 \tag{40}$$

which is unique up to an overall multiplicative constant.

By the symmetry of the full nonlinear equation (36), both $\delta_0(t)+\xi(t)$ and $-\delta_0(t+\pi)-\xi(t+\pi)$ must be solutions to Eq. (36). Since δ_0 is a symmetric solution, $\xi(t+\pi)$ satisfies the linearized equation. But since this solution is unique up to an overall multiplicative constant, we must have

$$\xi(t)=C\xi(t+\pi)\ , \tag{41}$$

so that

$$\xi(t)=C^2\xi(t+2\pi)\ . \tag{42}$$

Comparison of Eq. (40) with Eq. (42) shows that $\mu=+1$.

It follows that generically the period-doubling case $\mu = -1$ will not occur, and symmetric limit cycles in symmetric systems must first undergo a bifurcation producing a pair of nonsymmetrical limit cycles before a cascade of period-doubling bifurcations can occur. Many symmetric systems become chaotic in exactly this way.[4,10,17,25–29] We again emphasize that Eq. (8) does not possess this symmetry, and consequently the linear stability analysis allows us to predict directly the parameter value for the onset of period doubling.

This paper only scratches the surface of the rich dynamics exhibited by Eq. (8). The wide variety of dynamical behavior seen as one wanders through the three-dimensional parameter space offers a host of interesting problems to be tackled. The present work gives hope that not all of these will prove intractable.

ACKNOWLEDGMENTS

We would like to thank John David Crawford, Michel Devoret, Jeff Lerner, and especially Jim Swift for helpful discussions. K.W. and E. K. were supported by the California Space Institute under Grant No. CS13-83. E. K. also acknowledges support from the Alfred P. Sloan Foundation. The work by J. C. and R. F. M. was supported by the Director, Office of Energy Research, Office of Basic Energy Sciences, Materials Sciences Division of the U.S. Department of Energy under Contract Number DE-AC03-76SF00098.

[1]B. D. Josephson, Phys. Lett. 1, 251 (1962).
[2]V. N. Belykh, N. F. Pedersen, and O. H. Soerensen, Phys. Rev. B 16, 4860 (1977).
[3]R. Y. Chiao, M. J. Feldman, D. W. Peterson, B. A. Tucker, and M. T. Levinsen, in *Future Trends in Superconductive Electronics, (Charlottesville, 1978),* Proceedings of the Conference on Future Trends in Superconductive Electronics, AIP Conf. Proc. No. 44, edited by B. S. Deaver, C. M. Falco, J. H. Harris, and S. A. Wolf (AIP, New York, 1979).
[4]B. A. Huberman, J. P. Crutchfield, and N. H. Packard, Appl. Phys. Lett. 37, 750 (1980).
[5]N. F. Pedersen, O. H. Soerensen, B. Duelholm, and J. Mygind, J. Low Temp. Phys. 38, 1 (1980).
[6]R. L. Kautz, J. Appl. Phys. 52, 3528 (1981); 52, 6241 (1981).
[7]N. F. Pedersen and A. Davidson, Appl. Phys. Lett. 39, 830 (1981).
[8]M. J. Feldman and M. T. Levinsen, IEEE Trans. Magn. MAG-17, 834 (1981).
[9]P. M. Marcus, Y. Imry, and E. Ben-Jacob, Solid State Commun. 41, 161 (1982).
[10]D. D'Humieres, M. R. Beasley, B. A. Huberman, and A. Libchaber, Phys. Rev. A 26, 3483 (1982).
[11]E. Ben-Jacob, I. Goldhirsch, Y. Imry, and S. Fishman, Phys. Rev. Lett. 49, 1599 (1982).
[12]M. T. Levinsen, J. Appl. Phys. 53, 4294 (1982).
[13]M. Odyniec and L. O. Chua, IEEE Trans. Circuits Syst. CAS-30, 308 (1983); University of California (Berkeley) Memorandum Report No. UCB/ERL—M83/12 (1983) (unpublished).
[14]R. F. Miracky, J. Clarke, and R. H. Koch, Phys. Rev. Lett. 50, 856 (1983).
[15]R. F. Miracky and J. Clarke, Appl. Phys. Lett. 43, 508 (1983).
[16]J. Clarke, R. F. Miracky, J. Martinis, and R. H. Koch, *Proceedings of the Seventh International Conference on Noise in Physical Systems, Montpellier, France, 1983,* edited by M. Savelli, G. Lecoy, and J.-P. Nougier (North-Holland, Amsterdam, 1983), p. 117.
[17]S. Novak and R. G. Frehlich, Phys. Rev. A 26, 3660 (1982).
[18]R. H. Koch, R. F. Miracky, and J. Clarke (unpublished).
[19]D. W. Jordan and P. Smith, *Nonlinear Ordinary Differential Equations* (Oxford University, Oxford, 1977).
[20]J. Guckenheimer and P. J. Holmes, *Nonlinear Oscillations, Dynamical Systems and Bifurcation of Vector Fields* (Springer, New York, 1983).
[21]J. D. Crawford, Ph.D. thesis, University of California, Berkeley, 1983.
[22]P. Holmes, Proc. R. Soc. London, Ser. A 292, 419 (1979).
[23]E. Knobloch and K. Wiesenfeld (unpublished).
[24]James W. Swift and Kurt Wiesenfeld (unpublished).
[25]D. R. Moore, J. Toomre, E. Knobloch, and N.O. Weiss, Nature 303, 663 (1983).
[26]B. A. Huberman and J. P. Crutchfield, Phys. Rev. Lett. 43, 1743 (1979).
[27]E. Knobloch and N. O. Weiss, Phys. Lett. 85A, 127 (1981).
[28]L. N. DaCosta, E. Knobloch, and N. O. Weiss, J. Fluid Mech. 109, 25 (1981).
[29]M. R. E. Proctor and N. O. Weiss, Rep. Prog. Phys. 45, 1317 (1982).